

Predictive Handover Strategy in 6G and Beyond: A Deep and Transfer Learning Approach

Ioannis Panitsas, Akrit Mudvari, Ali Maatouk, Leandros Tassioulas

Department of Electrical Engineering, Yale University, New Haven, CT, USA

Emails: {ioannis.panitsas, akrit.mudvari, ali.maatouk, leandros.tassioulas}@yale.edu

Abstract—Next-generation cellular networks will evolve into more complex and virtualized systems, employing machine learning for enhanced optimization and leveraging higher frequency bands and denser deployments to meet varied service demands. This evolution, while bringing numerous advantages, will also pose challenges, especially in mobility management, as it will increase the overall number of handovers due to smaller coverage areas and the higher signal attenuation. To address these challenges, we propose a deep learning based algorithm for predicting the future serving cell utilizing sequential user equipment measurements to minimize the handover failures and interruption time. Our algorithm enables network operators to dynamically adjust handover triggering events or incorporate UAV base stations for enhanced coverage and capacity, optimizing network objectives like load balancing and energy efficiency through transfer learning techniques. Our framework complies with the O-RAN specifications and can be deployed in a Near-Real-Time RAN Intelligent Controller as an xApp leveraging the E2SM-KPM service model. The evaluation results demonstrate that our algorithm achieves a 92% accuracy in predicting future serving cells with high probability. Finally, by utilizing transfer learning, our algorithm significantly reduces the retraining time by 91% and 77% when new handover trigger decisions or UAV base stations are introduced to the network dynamically.

Index Terms—6G, Radio Access Network, Machine Learning

I. INTRODUCTION

Next-generation cellular networks will guarantee end-to-end low latency and high reliability, provide high data rate connectivity and increased capacity for broadband services, and support new types of end devices [1]. Additionally, Software-Defined Networking (SDN) and Network Function Virtualization (NFV) approaches will be fully adopted, ensuring control and user plane separation for better scalability, flexibility, and enabling the virtualization of different network layers [2]. Machine Learning (ML) is also expected to be integrated into critical parts of the network for closed loop control, optimization, and automation, further enhancing the network's efficiency and adaptability [3]. To satisfy the diverse Quality of Service (QoS) requirements, higher frequency bands in the spectrum will be utilized, including mmWave and THz waves, along with denser and more heterogeneous deployments of various cells with different capacities and access technologies. Moreover, in 6G cellular technology, a primary consideration will be the integration of non-terrestrial networks, including satellites and embedded base stations in Unmanned Aerial Vehicles (UAVs), alongside terrestrial networks for worldwide coverage and enhanced network capacity [4]. This will be particularly valuable in areas with limited infrastructure, where

they can also be deployed dynamically to efficiently manage traffic spikes during events with short-term high demand [5]. Mobile base stations will be a significant part of this network evolution, possessing the ability to change their location to maximize network performance. This mobility will be crucial for aligning network resources with varying demand patterns, enabling the system to efficiently allocate bandwidth and maintain QoS in dynamic environments.

A primary challenge in this heterogeneous cell deployment is managing user mobility effectively. Due to increased signal attenuation and smaller cell coverage, mobile nodes will frequently need to be handed over to new base stations, necessitating the establishment of fast and secure connections without service interruption. This issue could become a significant bottleneck, especially for services requiring end-to-end low latency when handover optimization algorithms are not applied. Classical approaches mainly monitor User Equipment (UE) channel quality measurements in the downlink channel, such as Reference Signal Received Power (RSRP) and Signal-to-Interference-plus-Noise Ratio (SINR), to initiate a handover request. While these approaches are fast and easy to implement, they lack capturing the current network state (such as network load and energy consumption).

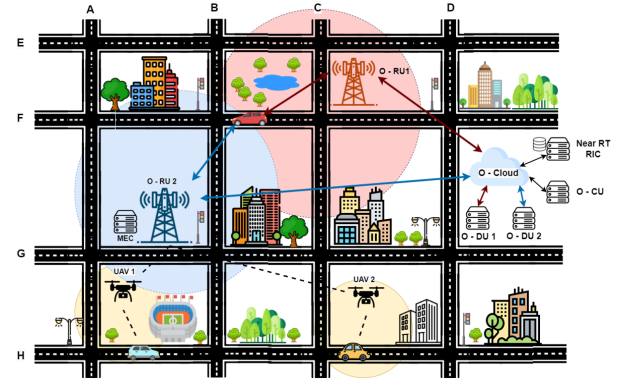


Fig. 1. Frequent handover requests occur in dense cell deployments at terrestrial or UAV base stations.

In next-generation cellular networks it is expected that the handover triggering event will become more complex for optimizing various network objectives simultaneously. For instance, when the received signal for a target cell is stronger than the serving cell, and the target cell has available resources and is energy-efficient to connect with it, then the UE can

initiate a handover request to this cell. Network operators can also introduce various new parameters to support, for example, network priorities and network slices, for better network performance [6]. In these cases, ML can be utilized to model the handover decision process, given its capability to adapt and learn from complex and dynamic network conditions. Numerous studies have explored the application of ML to predict handover events based on UE reported channel quality measurements and cell statistics [8] - [12]. The core idea is to forecast the handover triggering event in order to prepare the target base station for resource allocation for the UE. Proactively preparing the target base station can minimize Radio Link Failures (RLF) that occur when the handover decision is delayed and can reduce Handover Ping-Pongs (HOPP), where a UE frequently switches between serving base stations. For instance, the authors in [8] proposed a DL algorithm for minimizing the PPHOs and RLFs and they showed that their DNN achieved a better performance compared with the state-of-the-art algorithms. The authors in [9] designed and evaluated intelligent handover prediction models for 5G networks to ensure zero downtime during user transitions. In [10], the authors propose an ML-based algorithm for managing and forecasting handovers in mobile networks, while also detecting abnormal handovers to neighboring cells. Numerous research efforts also focused on managing handovers between users and UAV base stations. For instance, in [13], the authors examined the challenges in integrating mobile UAV base stations and analyzed handover management related issues. In [11], the authors proposed a Deep Reinforcement Learning (DRL) approach to minimize handover delay, interference, and radio resource utilization in an environment with UAVs and terrestrial base stations.

Recent innovations in the Open Radio Access Network (O-RAN) architecture, as defined by [14], enable the deployment of third-party ML applications in the RAN for enhancing network automation and management. In the O-RAN architecture, a base station is disaggregated into a Central Unit (CU), a Distributed Unit (DU), and a Radio Unit (RU), allowing flexibility in deployment and functionality. The CU further is disaggregated into a CU User Plane (CU-UP) and a CU Control Plane (CU-CP), managing user data traffic and control functions, respectively. Radio Intelligent Controllers (RICs) introduce programmable components facilitating closed-loop control and orchestration of the RAN using ML algorithms. Various research works also exist in the field of O-RAN by utilizing ML algorithms for handover management. For instance, the authors in [15] introduced “Roadrunner,” an O-RAN based algorithm enhancing 5G cell selection for better throughput and fairness, without altering existing devices or standards. In [12] the researchers proposed a DRL algorithm for intelligent connection management in O-RAN networks, aiming to optimize user-cell association and network load balancing.

Recognizing the gap in literature in O-RAN-based mobility management and acknowledging that handover decisions are becoming increasingly complex and dynamic for network

optimization, our main contributions in this work can be summarized as follows:

- We propose a deep and transfer learning-based algorithm that is compliant with the O-RAN architecture and can accurately predict the target cell over a predefined time window based on various dynamic events that may occur in the cellular network.
- We introduce a novel handover management architecture that can be deployed in a Near Real Time RIC Controller for real time decisions. Our architecture allows network operators to dynamically update the handover decision rules for network optimization and incorporate new UAV base stations for increased capacity, thereby enhancing network coverage while minimizing the retraining time and associated computation costs.
- We evaluate our framework using a simulated cellular network and compare its performance with classical supervised ML algorithms. We demonstrate that our framework can predict the target cell with 92% accuracy using a time window W of 70 measurements. Finally, we show that it reduces the retraining time by 91% when dynamic load balancing handover decision rules are incorporated and by 77% when new UAV base stations are introduced, respectively. To the best of our knowledge, we are the first to introduce the concept of transfer learning in handover management in the O-RAN environment.

The rest of the paper is organized as follows. Section II describes the classical handover procedure in 3GPP, and introduces the handover types in an O-RAN environment. Section III presents our predictive handover algorithm and Section IV provides the evaluation results. Lastly, Section V concludes our work.

II. BACKGROUND

A. The Classical Handover Procedure in 3GPP

Based on the Third Generation Partnership Project (3GPP) technical specification [16], each base station calculates a handover margin (HOM) value, which is then transmitted to all the UEs. If a UE detects that the RSRP from a neighboring base station exceeds the RSRP of its serving base station by at least this handover margin for a specified duration, known as the “Time To Trigger (TTT),” it generates and sends a measurement report to the serving base station. This report contains details on the RSRPs and SINRs of the neighboring base stations to its serving base station, signaling the need for a handover. The current serving base station evaluates the information to determine the best target base station to handover the UE to, completing thus the handover process. In the described algorithm, it is evident that there is no restriction preventing a UE from connecting to an overloaded base station, potentially leading to suboptimal QoS due to congestion. Consequently, handover decision-making needs to consider additional factors such as network load, UE mobility, and energy demands. Given these considerations, the process of initiating a handover becomes more complex due to its dependency on multiple parameters.

B. Types of Handover in O-RAN

Based on the disaggregated RAN architecture, 3GPP has introduced new types of handover [14] considering gNB-CU and gNB-DU implementations. Intra-gNB-DU handover occurs within the same gNB-DU, while an inter-gNB-DU and intra-gNB-CU handover involve transitions between different gNB-DUs under the same gNB-CU. Inter-gNB-CU handovers involve transfers between different gNB-CUs, executed via Xn or N2 interface. Figure 1 illustrates a scenario of an inter-gNB-DU and intra-gNB-CU handover, where cell 1 (O-RU1) is connected to O-DU1, and cell 2 (O-RU2) is connected to O-DU2, where both of the cells are managed by the same O-CU. This figure illustrates the process where the UE transitions from cell 1 to cell 2.

III. PREDICTIVE HANDOVER BASED ON DEEP AND TRANSFER LEARNING

In this work, we address the problem of forecasting the optimal target cell to which the UE will attach as it moves to the intersection of edge cells, formulating it as a multi-class classification problem. To predict the target cell, we utilize sequential channel quality measurements (RSRP and SINR) collected from the UE over a predefined time window size W , which are reported to the serving cell. The predictions will be made for the next time window size W based on the current window measurements. Additionally, we assume that the network operator can dynamically change the handover decision parameters and introduce new features, such as available Physical Resource Blocks (PRBs) and the number of users in each cell. Thus, the handover decision parameters can be dynamically changing and the decision will not be made solely on channel quality measurements. We consider two types of dynamic events that can occur in the network:

- 1) **Dynamic handover control parameters:** The network operator can dynamically change the handover decision parameters, e.g., UE channel quality, with additional parameters to ensure load balancing, energy efficiency, connection prioritization, etc., for optimizing different aspects of the network when handovers occur.
- 2) **Dynamic UAV base stations:** The network operator can dynamically incorporate new UAV base stations into the network for better coverage, network performance, and QoS for the end-users.

To address this multi-class classification problem and enable the incorporation of new dynamic handover decision rules, we introduce a framework that employs deep and transfer learning techniques. DL is a powerful tool, particularly effective at identifying and learning complex patterns within sequential data—crucial for tasks like predicting cell handover in telecommunications, where traditional ML models may fall short. DL models excel at learning and managing long-term dependencies, vital for forecasting network behavior and cell transitions. They autonomously discover useful representations for feature selection, enhancing the accuracy of handover predictions, and they can adapt to new patterns in

dynamic network environments, improving decision-making in cell handover processes. On the other hand, we employ transfer learning because it enables quick adaptation to new or changing tasks or environments by leveraging knowledge from previously trained models. Utilizing knowledge from previously trained models and transferring the learning weights from the old model, we can save training time and computational resources while maintaining a high prediction accuracy. In our case, we utilize transfer learning when new handover control parameters or new UAV base stations are introduced.

Our algorithm is UE-centric, and can be deployed as an xApp in a near-RT RIC for handover management. The near-RT RIC can collect and pre-process data from the E2 nodes (O-DU, O-CU) and forward them through the internal interface to the xApp. Our xApp leverages the E2SM-KPM service model from the E2 nodes for collecting user and cell specific Key Performance Metrics (KPM) in a periodic fashion for creating the time window W that will be used from our model for cell prediction. For near real time handover decisions, we assume that the O-DU nodes and the near-RT RIC are deployed in the edge cloud while the O-CU nodes are deployed in a regional cloud. Fig. 2 illustrates the deployment of our handover management xApp in the near-RT-RIC and the process of making handover decisions. Finally, we assume that the network operator can configure the sampling period time T_s for the UE and the cell measurements, thus our model can predict the future serving cell for a time window of $T_s \cdot W$.

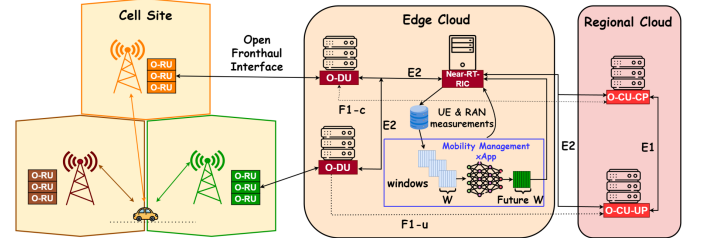


Fig. 2. Our proposed predictive handover algorithm is implemented as an xApp in the near-RT RIC. Our framework predicts a handover request to the green cell in the near future.

Our framework has three main components: the Encoder, the Stacked Long Short-Term Memory (S-LSTM) layers, and the Decoder, as illustrated in Fig. 3. The encoder encodes the input features to a higher dimension for additional expressiveness and changes its input size when a dynamic event occurs. It produces a fixed-size output that the S-LSTM layers use as input, and it is shared across all the LSTM cells. The core idea of introducing the encoder before the S-LSTM layers is that whenever a dynamic event occurs, it is more time-efficient to retrain the encoder compared to the complex structure of the LSTM cell and the S-LSTM layers when the dimension of the input size changes. Therefore, we expect that the weights of the S-LSTM layers do not change drastically with this architecture. The S-LSTM layers learn complex temporal patterns and extract useful features by forwarding their outputs to the next layer, which the decoder then uses. The decoder utilizes

the last hidden state of the last S-LSTM layer, and produces a probability distribution for all the cells that the UE scans in the network. Based on a predefined probability threshold, we can predict cell attachment in the next time window W with high accuracy. The encoder comprises three fully connected Multi-Layer Perceptrons (MLPs). There are two S-LSTM layers, and the decoder consists of a fully connected MLP followed by a softmax layer. The size of the sequence that the S-LSTM layers can process has been carefully selected to avoid the vanishing gradient problem. More details about the model architecture and the hyperparameters used can be found in Table I.

Algorithm 1 Data Labeling Algorithm

Inputs:

RSRP _{W,N} : RSRP vector of W time steps for N neighbors
PRB _{W,N} : PRB vector of W time steps for N neighbors
RSRP_{serv}: RSRP of serving cell
HOM: Handover Margin
Threshold_{dynamic}: Maximum dynamic threshold of PRB utilization in each cell

Output:

HandoverDecision _{N} : Decision vector for N cells

for $n = 1$ **to** N **do**

HandoverDecision _{n} \leftarrow 0

for $t = 1$ **to** W **do**

RSRPConditionMet \leftarrow true

if $RSRP_{t,n} \leq RSRP_{serv} + HOM$ **then**

RSRPConditionMet \leftarrow false

break

end if

end for

if RSRPConditionMet **and**

$\frac{1}{W} \sum_{i=1}^W PRB_{i,n} < Threshold_{dynamic}$ **then**

HandoverDecision _{n} \leftarrow 1

else

HandoverDecision _{n} \leftarrow 0

end if

end for

TABLE I
MODEL ARCHITECTURE

Encoder:

3-layer MLP (32, 16, 32 neurons)

S-LSTM Layers:

2 stacked layers, 32 input/hidden size

Decoder:

1-layer MLP, neurons equal to the number of cells

Activation:

ReLU

Training Parameters:

Window W : 70, Batch: 64, LR: 0.005,

Dropout: 0.5, Batch Normalization: Yes, Scaler: Standard

Loss: Cross-entropy, Optimizer: SGD

To train our model, we created datasets based on a simulated

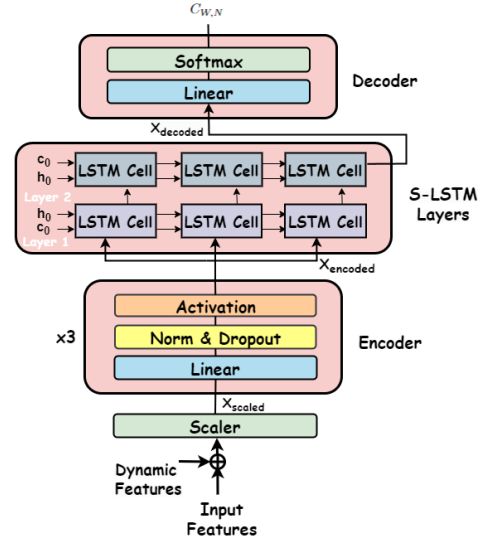


Fig. 3. Our model architecture consists of the Encoder, the S-LSTM layers, and the Decoder.

network environment, as illustrated in Table II. Initially, we generated a dataset in which the handover decision to a cell is made solely based on the UE-reported channel quality measurements. Subsequently, we created another dataset where the decision is influenced not only by the channel conditions but also by the availability of the target base station's radio resources, following our Data Labeling Algorithm (Algorithm 1). Considering different UE mobility scenarios, we generated approximately 200 distinct movement scenarios with varying UE velocity speeds close to the edge cells. This process resulted in a collection of 100,000 measurements, with a balanced number of classes across our data. We used 60% of the collected data for training our model, with the remaining 40% split equally between evaluation and testing. Hyperparameter tuning was conducted on the validation set to optimize model parameters, prevent overfitting, and enhance generalization on unseen data. More information about our implemented algorithm can be found in Algorithm 2.

IV. EVALUATION RESULTS

The performance of our proposed framework was evaluated by comparing it with three supervised ML algorithms: Random Forest (RF), MLP with one hidden layer of size 32, and a Gated Recurrent Unit (GRU) layer with input and hidden sizes of 32. Hyperparameter tuning was conducted for all the ML models. Initially, the performance comparison of our model utilized UE and cell-specific measurements in scenarios without dynamic events. From Table III, the accuracies of the RF and MLP models were relatively low at 64% and 69% respectively, while the accuracy of the GRU was 86%. The RF and MLP models could not exploit the long-term sequential dependencies of the measurements, while the GRU used the same optimal time window as our model (see Fig. 4). Our proposed model outperformed all of them with an accuracy of 92%, which was 6% higher than that of the GRU, 24% higher

TABLE II
SUMMARY OF CELLULAR NETWORK CONFIGURATION

Network Configuration

Cellular Network

Configuration: Urban Macrocell (UMa)
Macrocells: 7 in a hexagonal layout
Intersite Distance: 1000 m
Coverage Area: 2500 x 2500 m^2
UAV Base Station: Dynamically deployed, 200 x 200 m^2

Transmission Specs

Carrier Frequency: 4 GHz (Macro), 5 GHz (Micro)
Bandwidth: 20 MHz (Macro), 20 MHz (Micro)
Transmit Power: 35 dBm (Macro), 20 dBm (UAV)
Antenna Gain: 2 dB

Handover Parameters

Handover Margin (HOM): 3 dB
Time-To-Trigger (TTT): 100 ms
Maximum Cell Load (PRB Utilization): 0.8

Path Loss Models

Macrocell Model: NLOS: $PL_{NLOS} = 13.54 + 39.08 \log_{10}(d_{3D}) + 20 \log_{10}(f_c) - 0.6(h_{UT} - 1.5)$, $\sigma_{SF,NLOS}^2$: 6 dB
UAV Model: LOS: $PL_{LOS} = 28.0 + 22 \log_{10}(d_{3D}) + 20 \log_{10}(f_c)$, $\sigma_{SF,LOS}^2$: 4 dB

UE Parameters

Distributed UEs: R UEs with full buffer traffic model
Height: 1.5 m
Velocity: 60 km/h
Sensitivity: -110 dBm
Mobility Model: Manhattan, 50 m grid

than the MLP, and 28% greater than the RF. Fig. 4 illustrates our model's performance across different window sizes when initially our model was trained solely on UE Channel Quality Features (orange line), trained combined with UE Channel Quality Features and Cell Load Features (blue line), or trained initially with UE Channel Quality Features and dynamically new features were added to the model (pink line). Based on the results from Fig. 4, we selected an optimal window size equal to 70 as the accuracy did not improve anymore, and it was a good balance to avoid any issues with long-term dependencies. Figures 5, 6, 7 and 8 illustrate the training and testing losses before and after a transfer learning event occurs. Specifically, Figures 5 and 6 display the losses when our model is initially trained using only UE Channel Quality Features (orange line) or combined UE Channel Quality Features and Cell Load Features. At epoch 300 (green dashed line), a transfer learning event is initiated, introducing Dynamic Cell Load Features (pink line) and thus transferring all weights from the previous model and randomly initializing the new parameters. Initially, the training and testing losses increase from 0.28 to 0.42 and from 0.3 to 0.46 respectively when dynamic features are added, but eventually, the model converges near to the optimal training and testing loss like the model was trained initially with all the features and the retraining process only requires 25 epochs, saving approximately 91% of retraining time. Similarly, in Figures 6 and 7, the training and testing losses are illustrated before and after a transfer learning event occurs, i.e., a dynamic UAV base station is added to the

network. Initially, the training and testing losses increase from 0.21 to 0.91 and from 0.19 to 0.87 respectively, but eventually, the model converges near to the optimal training and testing loss like the model was trained initially with all the features and the retraining process only requires 70 epochs, saving approximately 77% of retraining time.

Algorithm 2 Cell Prediction using Transfer Learning

Inputs:

θ : Initial parameters of the model
 N : Number of neighboring cells
 $X_{W,M}$: Sequence of size W with M features at each time step.

Output:

$C_{W,N}$: Cell prediction over next W window

Initialize: Randomize model parameters θ

Training:

for $i = 1$ to K do

$X_{scaled} \leftarrow \text{Scaler}(X_{i,W,M})$
 $X_{encoded} \leftarrow \text{Encoder}(X_{scaled})$
 $X_{S-LSTM} \leftarrow \text{S-LSTM}(X_{encoded}, h, c)$
 $\hat{C}_{(i+1) \cdot W, N} \leftarrow \text{Decoder}(X_{S-LSTM})$
 $\min_{\theta} L(\theta) = - \sum_{i=1}^w \sum_{j=1}^N C_{(i+1) \cdot W, N}$
 $\times \log(\hat{C}_{(i+1) \cdot W, N}(\theta))$
via BPTT.
Update $\theta \leftarrow \theta - \eta \nabla_{\theta} L$.

end for

Inference:

if not new Dynamic Features or Dynamic UAV Event **then**
 $\hat{C}_{next W, N} \leftarrow f(X_{previous W, M}; \theta)$, where f maps input to output based on our model

else

Reconfigure model's structure
 $\theta' \leftarrow \theta \cup \{\text{randomized new parameters}\}$
Retrain model

end if

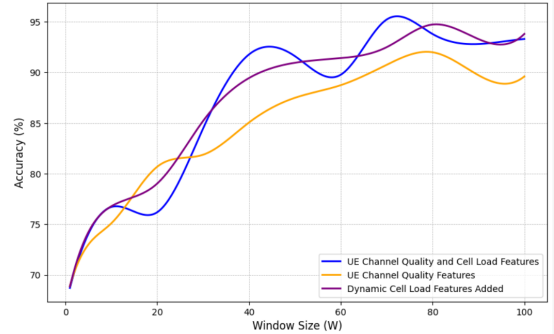


Fig. 4. Accuracy compared with different window sizes W .

V. CONCLUSION

In this paper, we propose a DL algorithm that predicts the future serving cell using sequential UE channel quality and dynamic features. Our method, acknowledging the need

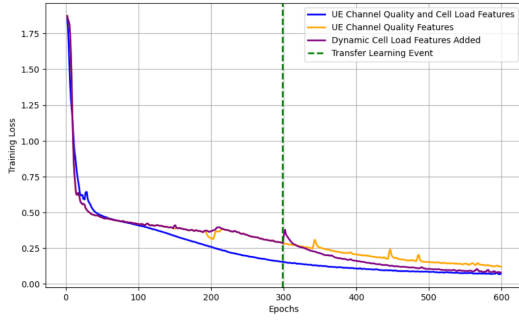


Fig. 5. Training Loss with dynamic features.

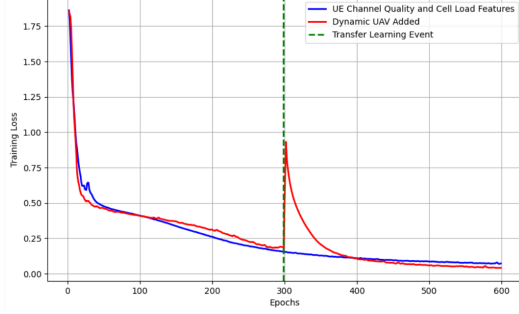


Fig. 7. Training Loss with dynamic UAVs.

TABLE III
SUMMARY OF MODEL PERFORMANCE

Model	Precision	Recall	F1 Score	Accuracy
RF	0.64 ± 0.03	0.67 ± 0.03	0.62 ± 0.04	$64\% \pm 3.5\%$
MLP	0.68 ± 0.02	0.68 ± 0.01	0.69 ± 0.02	$69\% \pm 2.1\%$
GRU	0.86 ± 0.06	0.87 ± 0.03	0.86 ± 0.05	$86\% \pm 0.8\%$
Our Model	0.92 ± 0.01	0.91 ± 0.01	0.93 ± 0.01	$92\% \pm 0.6\%$

for dynamic and new handover decisions for load balancing and energy efficiency, adapts easily to new decision rules or dynamic UAV base stations with minimal retraining through transfer learning. It aligns with O-RAN standards for deployment in a Near-RT RIC as an xApp using the E2SM-KPM service model. Results show that our model's predictive power reaches and maintains a 92% accuracy for predicting future cells, while reducing the retraining time by 91% and 77% for dynamic features and UAV base stations, respectively.

REFERENCES

- [1] W. Saad, M. Bennis and M. Chen, "A Vision of 6G Wireless Systems: Applications, Trends, Technologies, and Open Research Problems," in *IEEE Network*, vol. 34, no. 3, pp. 134-142, May/June 2020
- [2] F. Z. Yousaf, M. Bredel, S. Schaller and F. Schneider, "NFV and SDN—Key Technology Enablers for 5G Networks," in *IEEE Journal on Selected Areas in Communications*, vol. 35, no. 11, pp. 2468-2478
- [3] M. E. Morocho-Cayamcela, H. Lee and W. Lim, "Machine Learning for 5G/B5G Mobile and Wireless Communications: Potential, Limitations, and Future Directions," in *IEEE Access*, vol. 7, pp. 137184-137206, 2019
- [4] F. Rinaldi et al., "Non-Terrestrial Networks in 5G & Beyond: A Survey," in *IEEE Access*, vol. 8, pp. 165178-165200, 2020.
- [5] J. Lyu, Y. Zeng, R. Zhang and T. J. Lim, "Placement Optimization of UAV-Mounted Mobile Base Stations," in *IEEE Communications Letters*, vol. 21, no. 3, pp. 604-607, March 2017

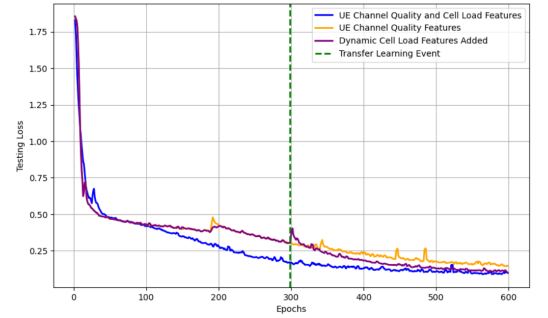


Fig. 6. Testing Loss with dynamic features.

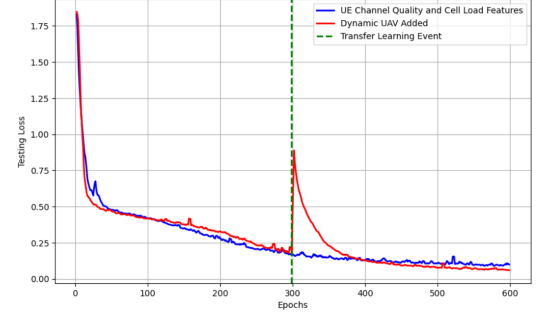


Fig. 8. Testing Loss with dynamic UAVs.

- [6] Y. Sun et al., "Efficient Handover Mechanism for Radio Access Network Slicing by Exploiting Distributed Learning," in *IEEE Transactions on Network and Service Management*, vol. 17, no. 4, pp. 2620-2633, Dec. 2020
- [7] M. S. Mollel et al., "A Survey of Machine Learning Applications to Handover Management in 5G and Beyond," in *IEEE Access*, vol. 9, pp. 45770-45802, 2021
- [8] Z. -H. Huang, Y. -L. Hsu, P. -K. Chang and M. -J. Tsai, "Efficient Handover Algorithm in 5G Networks using Deep Learning," *GLOBECOM 2020 - 2020 IEEE Global Communications Conference*, Taipei, Taiwan, 2020, pp. 1-6.
- [9] N. Uniyal et al., "Intelligent Mobile Handover Prediction for Zero Downtime Edge Application Mobility," *2021 IEEE Global Communications Conference (GLOBECOM)*, Madrid, Spain, 2021, pp. 1-6.
- [10] L. L. Vy, L. -P. Tung and B. -S. P. Lin, "Big data and machine learning driven handover management and forecasting," *2017 IEEE Conference on Standards for Communications and Networking (CSCN)*, Helsinki, Finland, 2017, pp. 214-219.
- [11] A. Azari, F. Ghavimi, M. Ozger, R. Jantti and C. Cavdar, "Machine Learning assisted Handover and Resource Management for Cellular Connected Drones," *2020 IEEE 91st Vehicular Technology Conference (VTC2020-Spring)*, Antwerp, Belgium, 2020, pp. 1-7
- [12] O. Orhan, V. N. Swamy, T. Tetzlaff, M. Nassar, H. Nikopour and S. Talwar, "Connection Management xAPP for O-RAN RIC: A Graph Neural Network and Reinforcement Learning Approach," *2021 20th IEEE International Conference on Machine Learning and Applications (ICMLA)*, Pasadena, CA, USA, 2021, pp. 936-941.
- [13] J. Angjo, I. Shayea, M. Ergen, H. Mohamad, A. Alhammadi and Y. I. Daradkeh, "Handover Management of Drones in Future Mobile Networks: 6G Technologies," in *IEEE Access*, vol. 9, pp. 12803-12823, 2021
- [14] O-RAN Working Group 1. (2021, July). O-RAN architecture description 5.00 (ORAN.WG1.O-RAN-Architecture-Description-v05.00 Technical Specification). O-RAN Alliance
- [15] E. Coronado, S. Siddiqui and R. Riggio, "Roadrunner: O-RAN-based Cell Selection in Beyond 5G Networks," *NOMS 2022-2022 IEEE/IFIP Network Operations and Management Symposium*, Budapest, Hungary, 2022, pp. 1-7.
- [16] ETSIA, "Procedures for the 5G System," *European Telecommunications Standards Institute (ETSI)*, Technical Specification (TS) 123 502, June 2018, version 15.2.0 Release 15